

Local spatial autocorrelation statistics quantify multi-scale patterns in distributional data: an example from the Maya Lowlands

L.S. Premo*

Department of Anthropology, University of Arizona, Tucson, AZ 85721, USA

Received 20 October 2003; received in revised form 24 November 2003; accepted 2 December 2003

Abstract

Three articles appearing in the *Journal of Archaeological Science* chronicle the application of spatial statistics to a set of 47 dated Classic Period monuments in the southern Maya Lowlands (*J. Archaeol. Sci.* 17 (1990) 197; *J. Archaeol. Sci.* 12 (1985) 377; *J. Archaeol. Sci.* 20 (1993) 705). Although previous studies demonstrate that tests of global spatial autocorrelation can inform interpretations of archaeological data, they do not provide the means to characterize local concentrations of spatially dependent values, or what Kvamme (*J. Archaeol. Sci.* 17 (1990) 203) called “the particular nature of [the global] trend”. Here, local Moran’s I_i and G_i^* statistics are applied to the same set of distributional data to quantitatively characterize spatial autocorrelation of terminal monument dates at the local, not global, scale. The results raise a number of local-scale hypotheses that, though undetected by previous global spatial analyses, might lead to a refined interpretation of the spatial distribution of dated monuments and, by extension, the reorganization of the Classic Maya. In a more general sense, the present application to dated Maya monuments serves as one example of how local spatial statistics can further strengthen distributional archaeological interpretations.

© 2003 Elsevier Ltd. All rights reserved.

Keywords: Local spatial autocorrelation; Spatial statistics; Spatial scale; Landscape signatures; Archaeological landscapes; Classic Maya

Spatial autocorrelation is a powerful technique for the analysis of spatial patterning in variate values which has been successfully applied in locational geography [3,5], and the method should find many relevant archaeological applications [20, p. 705].

1. Introduction

Williams’ [20] prediction that spatial autocorrelation statistics would assume a prominent role in quantitative archaeological analyses has yet to be realized. A search of the recent literature shows that spatial autocorrelation statistics have found few archaeological applications. Interestingly, one set of terminal long-count dates from Classic Maya monuments in the southern Lowlands has undergone the majority of the few archaeological spatial autocorrelation analyses. A termi-

nal long-count date refers to the most recent known stone monument construction event at a site. Although subject to modification via continuing archaeological investigation, terminal monument dates provide indicators of the years in which elites ceased to raise stone monuments at various geographic locations throughout the region. Because the cessation of this cultural practice has long been associated with the Classic Maya “collapse” [11], this set of data provides an opportunity to apply quantitative methods to archaeological research questions concerning the spatial organization of one of the most important social, economic, and political events in Maya culture history.

Others have realized the potential held by the distribution of dated monuments, and the results of their analyses are reviewed below. Three studies should be commended for addressing spatial issues with their quantitative assessments of the terminal long-count date distribution. In each of these cases, global spatial statistics were used to characterize spatial patterning at the scale of the entire southern Lowlands region. Although

* Corresponding author. Tel.: +1-520-621-2585; fax: +1-520-621-2088

E-mail address: lpremo@email.arizona.edu (L.S. Premo).

identifying a global trend is a necessary first step in exploratory spatial analysis, in many cases, quantifying localized patterns of spatial dependence is more important to formulating detailed, defensible archaeological interpretations.

This article introduces two local spatial statistics that were designed to elucidate how distance-defined clusters of values, called spatial neighborhoods, contribute to the global spatial structure of a distribution. The following analysis is an extension of the pioneering global spatial autocorrelation studies that have come before. In contrast to the results yielded by previous global analyses, however, local spatial statistical results provide an understanding of how individual dates compare to those within spatially defined neighborhoods as well as how localized subsets of dates influence the global spatial structure of the study area. Just as importantly, they allow us to quantitatively characterize landscape signatures that result from human behaviors that operate at various scales between that of the artifact and that of the geographic region.

2. Previous research

Frederick Bove [2] was among the first to comment on the global spatial structure displayed by terminal long-count dates of carved Lowland Classic Maya monuments. He used a series of polynomial trend surfaces to argue that the spatial distribution of terminal long-count monument dates supported neither a strong west-east trending cultural disintegration nor a hostile invasion by an enemy faction. According to Bove [2], numerous concentrations of positive trend surface residuals provided support for the hypothesis that the collapse was marked by a complicated process of socio-political decentralization and facilitated by destructive competition between feudal-like city-states. By independently identifying areas that could be interpreted as the hypothesized decentralized seats of socio-political power, his work dovetailed nicely with this popular model of the Classic Maya collapse [2,9].

Bove's spatial data soon reappeared in an ambitious article published by Whitley and Clark [19]. They employed a global spatial autocorrelation statistic to further investigate the spatial structure of the terminal long-count data. Spatial autocorrelation statistics test the degree to which the value of a particular attribute in one locale is similar to values of the same attribute in adjacent locales. According to Tobler's [17] so-called "First Law of Geography," the degree of similarity between the attribute values of two locales is inversely related to the distance between them. In other words, closer locales tend to be more similar than distant ones. Spatial data that behave this way exhibit positive spatial autocorrelation. On the other hand, when adjacent values are dissimilar (e.g., the colors of a chessboard),

spatial data is said to exhibit negative spatial autocorrelation. If values are randomly distributed across space, then the distribution altogether lacks spatial autocorrelation.

Whitley and Clark [19] were among the first to consider at length the role that spatial autocorrelation could play in quantitative archaeological analyses. Their introduction to global spatial autocorrelation statistics is straightforward and informative, and their application of Moran's I [10] to simulated archaeological data sets clearly illustrates the relationship between familiar visual patterns and less familiar spatial autocorrelation results. However, the authors failed to realize the full potential of Moran's I when they applied an area-based version to Bove's point-distributed data. As subsequent reanalyses argued, their decision to employ an area-based test of spatial autocorrelation reduced the information content of the long-count data such that the results could not disprove the null hypothesis (no spatial autocorrelation) at the conservative P -value of 0.05 [7,20]. As a result, Whitley and Clark [19, p. 390] conclude that their tests "fail to provide support for the notion that there was any [global] geographical pattern in the terminal distribution of Maya long-count dates", thereby contradicting Bove's earlier interpretation.

Taking issue with Whitley and Clark's application of the area-based test, Kvamme [7] applied a distance-based version of Moran's I to the same point-distributed terminal long-count data set. The most significant departure of Kvamme's analysis is an inverse distance weight matrix. According to this method, terminal dates located relatively close to one another are assigned heavier spatial weights than dates separated by greater distances. Unlike Whitley and Clark's area-based results, Kvamme's distance-based findings statistically support the interpretation that terminal dates of Maya monuments exhibit positive spatial autocorrelation at the global scale, or, as described above, that similar dates are nonrandomly clustered in close spatial proximity. Kvamme noted, however, that while his test indicates positive spatial autocorrelation at the global level, it does not describe the particular, localized details of that trend. In his own reanalysis, Williams [20] also made a point of the inability of global spatial autocorrelation tests to detect localized clusters of comparable long-count dates directly.

In a more recent attempt to characterize local spatial signatures in the Classic Maya Lowland monument data, Neiman [12] presented a trend surface estimated with local robust regression (loess) for 69 terminal long-count dates. He argued that the presence of localized ecological disasters caused by deleterious soil erosion in areas receiving the highest levels of rainfall [14] constitutes a viable explanatory model for the early discontinuation of monument building. In addition, the semi-variance of his loess surface residuals implies that

Late Classic political competition occurred at a relatively small scale. Neiman's estimate of polity size based on the semi-variance of terminal monument date trend surface residuals independently supports that which Houston [6] found with a nearest-neighbor distance analysis of 32 Late Classic sites containing emblem glyphs.

Of all the studies reviewed above, Neiman's [12] semi-variance approach is the only one that quantifies some local-scale details of the global trend. In this case, semi-variance calculations provide a measure of the dissimilarity that exists among loess residuals as a function of the distance between point pairs. Neiman effectively argues that when calculated for a sufficient range of distances, semi-variance can be used "to estimate the scale of political competition among monument building elites on the eve of the collapse" [12, p. 282]. However, because a variogram tracks the semi-variance that exists between *pairs of attribute values* located within a certain lag distance of each other rather than between a *target value and its spatial neighborhood of values*, it does not provide a measure of local spatial autocorrelation as defined by Anselin [1]. That is, a variogram does not provide for each instance an index that measures how similar its value is to all of the values located within a given radius, nor does it quantify each point pair's influence on the global spatial structure. It is possible that in some cases semi-variance results and local spatial autocorrelation results might overlap. However, one can devise an experimental spatial distribution from which pair-wise methods and neighborhood methods will yield different results. As advertised, Neiman's insightful application of the variogram informs us of the scale at which Maya Lowland elites demarcated their political catchments with carved monuments, but it does not provide a measure of local spatial autocorrelation for each long-count terminal date that accompanied them.

3. Introducing local spatial statistics: G_i^* and I_i

During the 1980s and early 1990s, when only global indices were available to archaeologists interested in applying spatial autocorrelation to distributional data, quantitative geographers were grappling with how to quantify local patterns of association. Their hard work produced methods capable of not only recognizing but also quantitatively characterizing patterns of spatial dependence at multiple scales. These quantitative methods are called local spatial statistics.

When challenged with the task of characterizing localized spatial patterns, Getis and Ord [4] responded with their family of G statistics. No longer wedded to the global pattern, local G statistics are free to characterize the spatial autocorrelation of attribute values located within a user-defined distance of each target value. Getis

and Ord admonish that when used in conjunction with Moran's I , local G statistics can "detect local 'pockets' of [spatial] dependence that may not show up when using global statistics" [4, p. 190]. Local G statistics are appropriate for any spatial distribution composed of n instances, $i=1, \dots, n$, each of which is associated with a known Cartesian coordinate and a value x_i , taken from the non-categorical variable X . Following Getis and Ord [4], local G statistics are defined as:

$$G_i^*(d) = \frac{\sum_j w_{ij}(d)x_j}{\sum_j x_j} \quad (1)$$

and

$$G_i(d) = \frac{\sum_{j \neq i} w_{ij}(d)x_j}{\sum_{j \neq i} x_j} \quad (2)$$

where w_{ij} is a spatial weight matrix capable of accommodating binary (i.e., ones for all neighbors j within lag distance d of i and zeros for all locations greater than d from i) or non-binary (i.e., inverse distance, squared inverse distance, etc.) weights for each instance pair. The spatial weight matrix used in the present analysis is binary. For the purposes of this paper, the term *neighborhood* simply refers to the subset of adjacent sites j that fall within lag distance d of each i ; it is strictly a spatial term and implies nothing as to the socio-economic obligations that might have existed between sites considered to be *neighbors* or *neighboring*. The numerator is the summation of all x_j within d of i and the denominator is the summation of all x . G_i^* has the further stipulation that j cannot equal i , thereby excluding the target value x_i from numerator and denominator summations. Because the G_i^* statistic includes the target value in calculations it lends itself more appropriately to most archaeological research endeavors and will be the only G statistic discussed further here. G_i^* is positive when the sum of x_j within d of i is relatively large, negative when the sum of x_j within d of i is relatively small, and approximates zero when the sum of x_j within d of i is intermediate by comparison [4].

Just a few years after Getis and Ord published their G statistics, Anselin [1] introduced a more powerful class of spatial statistics called Local Indicators of Spatial Association (LISA), which includes a local adaptation of Moran's I (I_i). Like its global predecessor, local I_i measures the degree to which a target value is similar to the values displayed by adjacent locales. Unlike global I , however, the local version measures the similarity between each target value and the values within its neighborhood. Consequently, each target i receives an I_i that measures the degree of similarity that exists between its value and those of its spatially defined neighbors j . Local Moran's I_i is appropriately applied to any spatial distribution composed of n instances, $i=1, \dots, n$, each of which is associated with a known Cartesian coordinate and a value x_i , taken from the non-categorical variable

X . After Anselin [1, Equation 12], local Moran's I_i is defined as:

$$I_i = (z_i/m_2) \times \sum_j w_{ij} z_j \quad (3)$$

where z_i and z_j are deviations from the mean of variable X , $m_2 = \sum_i (z_i^2/n)$ as a second moment, and w_{ij} is a binary spatial weight matrix in which each pair of neighbors is assigned a one and each non-neighbor pair is assigned a zero. Local Moran's I_i is large and positive when x_i is similar to adjacent values x_j ; large and negative when x_i and neighboring values x_j are dissimilar; and approximates zero when no spatial autocorrelation exists between x_i and neighboring x_j [1,4].

To summarize, G_i^* and local Moran's I_i characterize two fundamentally different aspects of spatial distributions. The former is a relative measure of the sum of the values that exist within a target's neighborhood. G_i^* does not reveal how similar or dissimilar the attribute value x_i is to neighboring x_j . Alternatively, local Moran's I_i is a measure of the degree to which the attribute value x_i is similar (or dissimilar) to neighboring x_j . Local Moran's I_i does not address whether the sum of a neighborhood's values is relatively high or relatively low in comparison to those of other neighborhoods. I submit that when used in tandem local Moran's I_i and G_i^* can aid distributional archaeological interpretations by (1) quantitatively characterizing concentrations of comparable attribute values at multiple scales and (2) determining whether clustered values are greater than, equal to, or less than those in other target values' neighborhoods. To illustrate this potential, the next section applies I_i and G_i^* to an updated edition of Bove's terminal long-count data set.

4. Spatial data and methods

Table 1 presents the spatial data used in this analysis. Note that it includes the same 47 sites that Bove [2], Whitley and Clark [19], Kvamme [7], and Williams [20] analyzed. As Neiman [12] recently reported, since Bove's study many of the original terminal monument dates have been updated and others have been added. This exercise includes those revisions to the original assemblage of 47 sites. Williams' [20] methodology was employed to obtain coordinate locations for each of the Classic Maya sites in the study area. This procedure involved measuring the locations of the 47 sites, as presented by Whitley and Clark [19, Figure 3], to the nearest 0.5 millimeter and converting those measurements into kilometers north of and kilometers east of the southwest datum. Site coordinates have been included in this report in hopes that interested researchers will take this opportunity to experiment with the local spatial autocorrelation analysis introduced above and detailed below.

Despite the fact that local spatial statistics display a unique potential to investigate location-based hypotheses, few tools exist for applying them to archaeological data. Fortunately, Sawada [15] has provided a Visual Basic for Applications add-in for Excel, called Rookcase, which serves admirably both for education and application. This free extension provides a user-friendly tool that enables archaeologists to explore for both global and local spatial autocorrelation in area-based and point-based data within the confines of a familiar computing environment. The present analysis made exclusive use of Rookcase to calculate standardized I_i and standardized G_i^* scores at multiple scales for the terminal long-count data. Anselin [1] and Sokal et al. [16] explain that to redefine a raw I_i statistic as a standard variate under the hypothesis of total randomization, an expected value,

$$E[I_i] = -w_i/(n-1) \quad (4)$$

with $w_i = \sum_{j \neq i} w_{ij}$ the sum of i th's row elements (spatial weights), is subtracted from the raw statistic and the resulting quotient is divided by the square root of the variance,

$$\begin{aligned} \text{var}(I_i) = & [\sum_{j \neq i} w_{ij}^2 (n - b_2)/(n - 1)] \\ & + [(((\sum_{j \neq i} w_{ij})^2 - \sum_{j \neq i} w_{ij}^2) \times (2b_2 - n)) / \\ & ((n - 1) \times (n - 2))] - [-w_i/(n - 1)]^2 \end{aligned} \quad (5)$$

with $b_2 = \sum_i (z_i^4/n)/m_2^2$. Similarly, Ord and Getis [13] and Sokal et al. [16] redefine the G_i^* statistic as a standard variate under total randomization by subtracting from it an expected value,

$$E[G_i^*] = w_i^*/n \quad (6)$$

then dividing the resulting quotient by the square root of the variance,

$$\begin{aligned} \text{var}(G_i^*) = & [(w_i^* (n - w_i^*)) \times ((\sum_j x_j^2/n) - ((\sum_j x_j/n)^2))] / \\ & [(n^2 (n - 1) \times ((\sum_j x_j/n)^2))] \end{aligned} \quad (7)$$

where $w_i^* = \sum_j w_{ij}(d)$ the sum of i th's row elements (spatial weights), this time including w_{ii} . Rookcase calculates raw scores as well as standard variates for both local spatial statistics. Although they pose greater mathematical challenges, the standardized versions of local spatial statistics yield both negative and positive scores for data composed entirely of non-negative values, a characteristic that makes both interpretation and graphical presentation more intuitive. While consideration of raw statistics does not materially change conclusions, in the interests of convenience and clarity, only standardized results will be discussed throughout the remainder of this paper.

Table 1
Classic Period Lowland Maya terminal monument long-count dates

Site number ^a	Site name ^a	Northing (km) ^b	Easting (km) ^b	Monument ^c	Long-count date ^c	Date (AD) ^c
1	Aguas Calientes	194	239	Stela 1	9.18.0.13.18	791
2	Aguateca	171	252	New Stela	9.18.3.0.17	793
3	Altar de Sacrificios	184	218	Stela 15	9.17.0.0.0	771
4	Benque Viejo	248	371	Stela 1	10.1.0.0.0	849
5	Bonampak	210	158	Murals	9.17.15.12.10	792
6	Calakmul	355	294	Stela 64	9.19.0.0.0	810
7	Cancun	132	268	Stela 1	9.18.10.0.0	800
8	Caracol	208	369	Stela 17	10.1.0.0.0	849
9	Chinkultic	145	87	Stela 1	10.0.15.0.0	844
10	Comitan	156	45	Stela 1	10.2.5.0.0	874
11	Copan	6	371	Altar L	9.19.11.14.5	822
12	El Caribe	190	232	Stela 2	9.17.10.0.0	780
13	El Cayo	248	142	New	9.18.1.12.16	792
14	El Palmar	358	348	Stela 41	10.2.15.0.0	884
15	Ixkun	190	335	Stela 5	9.18.10.0.0	800
16	Ixlu	229	313	Stela 2	10.2.10.0.0	879
17	La Amelia	184	232	Panel 1	9.18.17.1.13	807
18	La Florida	23	395	Stela 7	9.16.15.0.0	766
19	La Honradez	297	355	Stela 4	9.18.0.0.0	790
20	La Mar	248	129	Stela 2	9.18.15.0.0	805
21	La Milpa	326	381	Stela 7	9.17.10.0.0	780
22	La Muneca	369	329	Stela 1	10.3.0.0.0	889
23	Lubaantun	156	387	Altar 2	9.18.0.0.0	790
24	Machaquila	168	294	Stela 5	10.0.10.17.5	841
25	Morales	335	119	Stela 1	9.16.5.0.0	756
26	Naachtun	326	303	Stela 10	10.16.10.0.0	761
27	Nakum	258	339	Stela D	10.1.0.0.0	849
28	Naranjo	252	355	Stela 32	9.19.10.0.0	820
29	Oxpemul	381	300	Stela 7	10.0.0.0.0	830
30	Palenque	295	65	Tablet 96	9.17.13.0.7	783
31	Piedras Negras	258	142	Altar 3	9.19.0.0.0	810
32	Polol	216	252	Stela 1	9.18.0.0.0	790
33	Pusilha	135	368	Stela E	9.15.0.0.0	731
34	Quen Santo	132	90	Stela 2	10.2.10.0.0	879
35	Quirigua	45	374	Temple 1	9.19.0.0.0	810
36	Seibal	182	271	Stelae 18, 20	10.3.0.0.0	889
37	Tayasal-Flores	232	287	Stela 1	10.2.0.0.0	869
38	Tikal	261	313	Stela 11	10.2.0.0.0	869
39	Tila	226	8	Stela A	10.0.0.0.0	830
40	Tonina	232	60	Monument 101	10.4.0.0.0	909
41	Tzmin Kax	213	377	Altar 1	10.0.5.0.0	835
42	Uaxactun	281	315	Stela 12	10.3.0.0.0	889
43	Ucanal	223	334	Stela 4	10.1.0.0.0	849
44	Uxul	332	277	–	9.16.0.0.0	751
45	Xultun	290	339	Stela 10	10.3.0.0.0	889
46	Yaxchilan	226	171	Lintel 10	9.18.17.13.14	808
47	Yaxha	248	335	Stela 31	9.18.5.16.4	796

^aFrom Bove [2, Table 1].

^bDerived from Whitley and Clark [19, Figure 3].

^cFrom Neiman [12, Table 15.1].

Standardized I_i and G_i^* variates were calculated for lag distances up to and including 200 km at 25 km intervals (Table 2). The results of the 75 km spatial lag were interpreted for two reasons. First, given the spatial distribution of the dated monuments, this particular lag distance provides the highest resolution at which each site belonged to a neighborhood composed of at least one other site (i.e., there is no “neighborhood” com-

posed only of the target site). Second, this lag distance approximates the spatial lag at which the sill is apparent in the semi-variance of Neiman’s [12] loess trend surface residuals. Neiman used the location of the sill to argue that the average distance over which Classic Period polities competed was roughly 65 km ([12, Figure 15.6]). Depending on the spatial structure of one’s data, local spatial autocorrelation results can be highly sensitive to

Table 2
Standardized I_i and G_i^* variates at lag distances from 25 to 200 km. Note that “–” is reported for sites that possess zero neighbors

Site	Date (AD)	I_i (25)	G_i^* (25)	I_i (50)	G_i^* (50)	I_i (75)	G_i^* (75)	I_i (100)	G_i^* (100)	I_i (125)	G_i^* (125)	I_i (150)	G_i^* (150)	I_i (175)	G_i^* (175)	I_i (200)	G_i^* (200)
1	791	1.054	-1.621	0.801	-1.194	0.703	-0.664	0.640	-0.429	0.633	0.006	0.698	-0.583	0.793	-0.592	1.122	1.028
2	793	-0.548	0.342	-0.244	-1.093	-0.225	-0.664	-0.169	-0.224	-0.115	-0.487	-0.057	0.102	-0.027	-0.493	-0.013	-0.698
3	771	1.406	-1.621	1.135	-1.948	0.922	-1.557	0.854	-1.141	0.804	-0.469	0.814	0.541	0.985	0.802	1.148	-0.361
4	849	0.003	0.435	0.049	0.915	0.081	2.127	0.096	1.834	0.129	1.531	0.160	1.059	0.201	0.279	0.201	0.279
5	792	0.231	-0.700	0.162	-1.049	0.149	-1.490	0.151	-1.915	0.167	-0.045	0.189	-0.426	0.219	0.319	0.282	0.384
6	810	-	-	0.046	-0.705	0.052	-0.026	0.078	0.847	0.097	1.118	0.118	1.616	0.146	1.970	0.240	0.132
7	800	-	-	0.031	-0.405	0.062	-0.868	0.073	-1.224	0.097	-0.992	0.146	-0.682	0.189	-0.161	0.254	-0.486
8	849	0.226	0.682	0.147	0.740	0.150	0.102	0.169	1.606	0.188	1.331	0.218	0.213	0.269	0.136	0.306	-0.310
9	844	0.726	1.324	0.535	1.810	0.535	1.810	0.410	2.065	0.338	1.195	0.326	0.627	0.320	-0.508	0.330	-0.823
10	874	-	-	0.022	1.242	0.031	1.810	0.046	2.474	0.057	1.718	0.078	0.722	0.082	0.318	0.102	-0.767
11	822	-	-	0.031	-0.895	0.031	-0.895	0.031	-0.895	0.031	-0.895	0.031	-1.859	0.052	-2.077	0.062	-1.858
12	780	1.279	-1.621	0.965	-1.194	0.818	-0.746	0.782	-0.495	0.741	-0.179	0.785	-0.350	0.889	-0.493	1.070	-0.361
13	792	0.341	-0.772	0.269	-1.071	0.269	-1.071	0.234	-1.397	0.232	-1.888	0.250	-0.360	0.277	-0.133	0.327	0.045
14	884	2.302	2.147	1.661	1.212	0.986	0.555	0.909	0.489	0.816	0.975	0.794	1.921	0.795	1.724	0.809	2.105
15	800	-	-	0.052	1.248	0.097	1.396	0.123	1.025	0.152	0.553	0.166	-0.124	0.207	-0.441	0.269	-0.562
16	879	0.881	1.406	0.411	1.421	0.368	2.956	0.383	1.438	0.423	-0.601	0.468	0.122	0.537	-0.345	0.587	-0.604
17	807	0.640	-1.771	0.554	-1.194	0.483	-0.746	0.468	-0.495	0.461	-0.635	0.491	-0.329	0.590	-0.493	0.724	-0.122
18	766	-	-	0.031	-0.895	0.031	-0.895	0.031	-0.895	0.039	-1.859	0.046	-2.019	0.052	-2.077	0.073	-1.370
19	790	-1.115	0.600	-0.481	0.889	-0.323	1.114	-0.220	2.050	-0.203	1.939	-0.175	2.098	-0.148	0.765	-0.133	0.188
20	805	0.285	-0.772	0.229	-1.071	0.217	-0.116	0.206	-1.018	0.212	-0.767	0.219	-1.155	0.232	-0.827	0.276	-0.161
21	780	0.000	0.000	0.031	-0.134	0.046	1.354	0.092	1.505	0.118	1.786	0.128	1.939	0.140	1.513	0.166	1.307
22	889	2.302	2.147	1.385	1.523	1.043	-0.410	0.909	0.489	0.827	0.793	0.796	1.845	0.793	1.872	0.803	1.970
23	790	-	-	0.022	-2.001	0.046	-1.092	0.062	-0.232	0.097	0.484	0.140	1.014	0.181	-0.164	0.189	-0.583
24	841	-	-	0.046	0.179	0.082	0.249	0.118	-0.509	0.140	0.310	0.173	0.198	0.198	-0.915	0.286	-1.710
25	756	-	-	-	-	0.022	-1.704	0.046	-1.728	0.057	-0.802	0.062	-1.018	0.073	-1.435	0.128	-1.897
26	761	-	-	0.039	-0.882	0.073	1.211	0.102	1.504	0.118	1.616	0.146	1.970	0.198	1.104	0.269	-0.286
27	849	-0.251	0.016	-0.072	2.161	-0.035	2.427	-0.006	0.895	0.045	1.656	0.087	0.279	0.095	0.188	0.124	-0.345
28	820	0.027	0.344	0.075	2.344	0.086	2.427	0.096	1.631	0.146	1.439	0.192	0.627	0.201	0.279	0.211	0.188
29	830	-	-	0.031	0.886	0.052	-0.026	0.062	0.210	0.078	0.847	0.097	1.118	0.118	1.616	0.146	1.086
30	783	-	-	-	-	0.031	-0.215	0.057	-0.597	0.057	-0.597	0.073	-0.436	0.082	0.203	0.092	-0.471
31	810	0.229	-0.772	0.202	-0.835	0.188	-1.071	0.174	-1.018	0.179	-2.099	0.204	-0.360	0.232	-0.073	0.291	0.528
32	790	-	-	0.062	-0.709	0.073	-0.022	0.118	0.391	0.166	0.057	0.217	-1.149	0.269	-0.489	0.354	0.425
33	731	-	-	0.022	-2.001	0.039	-1.370	0.062	-0.576	0.102	-0.304	0.146	-0.244	0.173	0.117	0.181	-0.164
34	879	0.726	1.324	0.726	1.324	0.535	1.810	0.535	1.810	0.348	1.510	0.326	0.627	0.320	-0.508	0.326	-0.388
35	810	-	-	0.031	-0.895	0.031	-0.895	0.039	-1.859	0.046	-2.019	0.057	-1.763	0.078	-0.793	0.097	-0.414
36	889	-1.006	0.649	-0.387	-0.541	-0.253	-0.131	-0.227	0.035	-0.144	0.027	-0.115	-0.417	-0.095	-1.258	-0.070	0.002
37	869	-	-	0.046	1.612	0.102	1.196	0.140	1.101	0.166	0.333	0.254	-0.345	0.269	-0.489	0.286	-1.060
38	869	1.757	1.900	0.734	2.681	0.661	1.726	0.634	1.385	0.690	1.244	0.753	0.188	0.825	-0.345	0.857	-0.489
39	830	-	-	-	-	0.022	1.587	0.039	1.320	0.057	1.634	0.068	1.136	0.082	0.203	0.082	0.203
40	909	-	-	-	-	0.039	0.499	0.062	0.679	0.082	0.203	0.082	0.203	0.087	-0.175	0.107	-0.973
41	835	0.226	0.682	0.147	0.740	0.148	0.838	0.169	1.606	0.178	1.752	0.225	0.635	0.269	0.136	0.293	-0.204
42	889	1.757	1.900	0.765	0.820	0.661	1.362	0.634	1.672	0.660	1.836	0.703	1.042	0.798	-0.112	0.857	-0.489
43	849	0.881	1.406	0.380	1.804	0.368	3.228	0.379	1.405	0.423	-0.601	0.455	0.213	0.482	0.188	0.560	-0.448
44	751	-	-	0.031	-1.928	0.057	0.654	0.078	1.389	0.112	1.442	0.128	1.117	0.240	0.132	0.240	0.132
45	889	-1.115	0.600	-0.434	1.428	-0.274	1.141	-0.211	2.093	-0.196	1.724	-0.158	1.457	-0.138	0.279	-0.125	-0.112
46	808	0.231	-0.700	0.153	-1.071	0.147	-1.814	0.151	-2.315	0.171	-0.530	0.200	0.277	0.260	-0.025	0.323	0.377
47	796	-0.225	0.016	-0.070	2.512	-0.023	2.427	0.011	1.955	0.076	0.697	0.098	0.279	0.107	0.188	0.136	-0.345

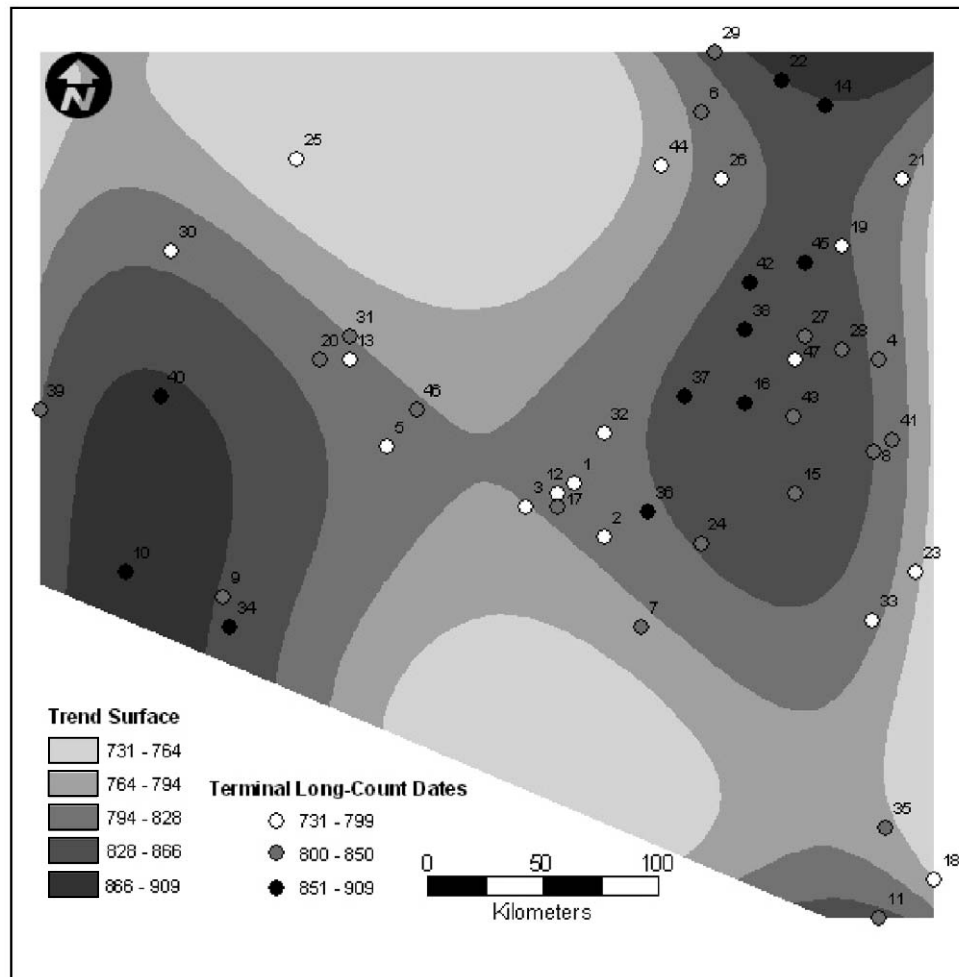


Fig. 1. Fourth order trend surface with terminal long-count date locations. Map values are in years AD. Sites are numbered consecutively and identified by name in Table 1.

variation in lag distance. Thus, it is strongly advised to systematically explore a range of lag distances for the presence of patterns at multiple scales before deciding on the results of one or more to interpret.

5. Results

Fig. 1 provides a fourth order polynomial trend surface for the updated Classic Maya monument data. Terminal long-count date locations (sites) are numbered as they are in Table 1. Note that this trend surface looks similar to Bove's fourth order trend surface ([2, Figure 6]). Apparent clusters of more recent terminal long-count dates sit atop the four "peaks" of the trend surface, while many of the earlier terminal dates reside below in the "valley." However, as discussed above, this global polynomial trend surface cannot elucidate multi-scale spatial manifestations. Enter local spatial autocorrelation statistics.

Fig. 2 presents standardized I_i variates at a lag distance of 75 km. In this case, I_i is an index of the similarity between a target long-count date x_i and the date(s) x_j at the location(s) j within 75 km of i . Large positive I_i scores are indicative of positive local spatial autocorrelation, where neighboring sites display terminal dates that are similar to that of the target site. These scores mark spatially defined concentrations of comparable terminal dates—the very spatial structure that global spatial autocorrelation tests and semi-variance analyses cannot identify. Twelve such scores, nested into four larger regions, can be observed in Fig. 2. Many of these scores identify neighborhoods composed of sites where elites erected monuments well into the 9th century AD. However, some positive I_i scores identify neighborhoods composed of sites with early terminal monument dates. One must consult a target's G_i^* result to distinguish between these two possibilities; positive G_i^* scores are indicative of the former and negative G_i^* scores signify the latter.

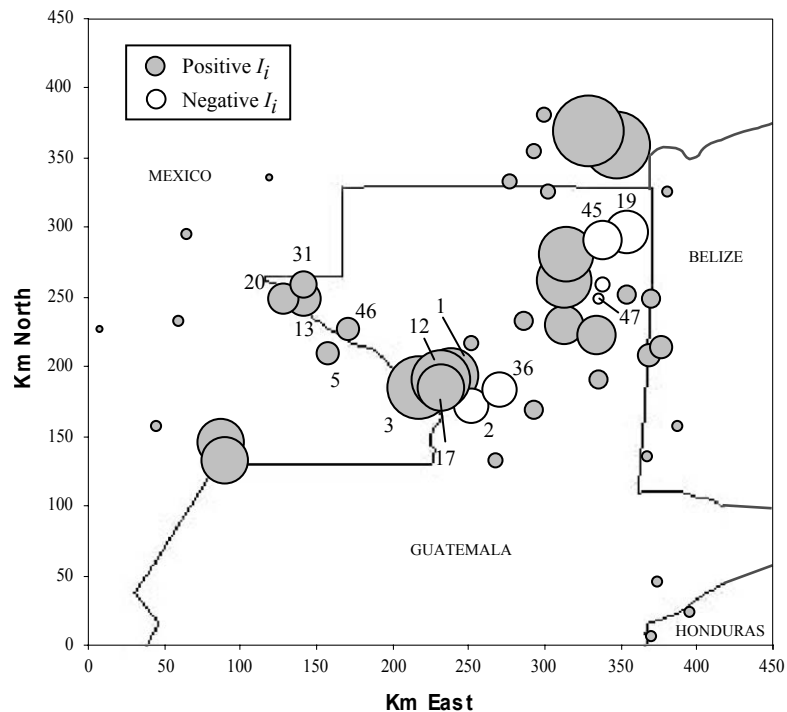


Fig. 2. Bubble graph of standardized local Moran's I_i scores at a lag distance of 75 kilometers. Shaded bubbles represent positive I_i scores, white bubbles represent negative I_i scores, and bubble area is proportional to $|I_i|$. Sites discussed in the text are labeled with their site number from Table 1. Contemporary political boundaries appear in the background.

Sites assigned negative I_i scores possess terminal long-count dates that are quite dissimilar from those of their neighbors. In this context, one possible interpretation of negative I_i scores is that they identify sites whose elites fled or ceased to erect monuments while those residing in neighboring sites continued the practice for decades. This might have been the case for Aguateca (2), La Honradez (19), and Yaxha (47), given their negative I_i scores, positive G_i^* scores, and early terminal dates. Alternatively, when combined with a late terminal date, large negative I_i scores can be interpreted as identifying the locations of decentralized seats of power where elites maintained the authority to continue to erect monuments for many decades after inhabitants of neighboring sites discontinued the cultural practice, or as identifying locales where attempts were made to re-establish socio-political control in previously abandoned regions. The local spatial autocorrelation results of Seibal (36) and Xultun (45) are more consistent with one of these latter interpretations.

It is important to reiterate that in the cases of both positive and negative I_i scores, local Moran's I_i alone provides no additional information that can be used to judge which of the alternative interpretations is most accurate. As demonstrated above, in order to distinguish between possible interpretations each site's original terminal date and/or its G_i^* score also must be considered. And, as I show below, the same principle holds true for G_i^* scores; each site's original terminal date and/or its I_i

score also must be considered before crafting a defensible interpretation. Therein lies the utility of using these two quantitative methods in concert. Alone, neither provides a complete characterization of a local spatial concentration.

Fig. 3 presents standardized G_i^* scores at a lag distance of 75 km. In this context positive scores are indicative of neighborhoods composed (mostly) of sites possessing late terminal long-count dates, negative scores signify neighborhoods composed (mostly) of sites with early terminal long-count dates, and scores near zero identify neighborhoods whose terminal long-count dates when summed are intermediate by comparison. Note that neighborhoods composed either entirely of intermediate values or an even mix of low and high values can provide G_i^* scores near zero. Local Moran's I_i scores can be used to distinguish between these two alternatives.

Given the results presented by Fig. 3 it is clear that a northwest to southeast linear arrangement of negative G_i^* scores bisects two regional aggregates of large positive scores. The linear arrangement of negative G_i^* scores indicates that, for the most part, elites in the central and southeastern sections of the study area ceased to raise monuments much earlier than those to the east and west. Additionally, when interpreted in conjunction with I_i scores, they also imply that in some cases entire neighborhoods of central sites stopped raising monuments nearly contemporaneously. The central neighborhood

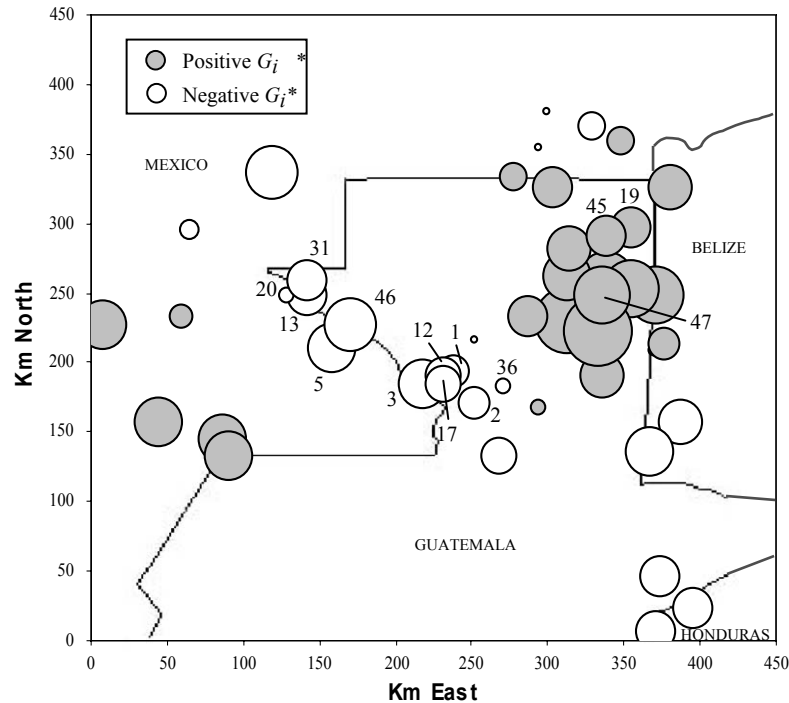


Fig. 3. Bubble graph of standardized G_i^* scores at a lag distance of 75 kilometers. Shaded bubbles represent positive G_i^* scores, white bubbles represent negative G_i^* scores, and bubble area is proportional to $|G_i^*|$. Sites discussed in the text are labeled with their site number from Table 1. Contemporary political boundaries appear in the background.

composed of Aguas Calientes (1), Altar de Sacrificios (3), El Caribe (12), and La Amelia (17), each of which possesses a relatively large positive I_i and a negative G_i^* score, provides a good example of this neighborhood-scale spatial signature. The same pattern is apparent, albeit slightly less distinct, in a nearby neighborhood composed of Bonampak (5), El Cayo (13), La Mar (20), Piedras Negras (31), and Yaxchilan (46). These quantitative results raise interesting questions: why would neighboring sites abandon monument building at approximately the same time, and what does the scale of this archaeological landscape signature tell us about the human behaviors responsible for the pattern?

Neiman [12] used rank correlations between local robust regression trend surface residuals and regional rainfall data [14] to argue that this type of early, large-scale abandonment is best explained by disastrous erosion events that are thought to have plagued the central region of the southern Maya Lowlands during the Classic Period. The local spatial autocorrelation results obtained here also identify central sites as the first to stop building monuments, but socio-political pressures cannot be ruled out by these findings alone. For example, although erosion might have been a detriment to everyday life in the central southern Lowlands, the ultimate reason for this area's abandonment could have been due to social pressures associated with living in contested territory. In addition to identifying early monument cessation, the local spatial statistics also

reveal the location, composition, and size of the neighborhoods that seem to have been affected (or responded) in similar fashion. As Kvamme [8] demonstrates, even when applied to spatial data, conventional statistics, such as Pearson's r and Spearman's r_s , cannot accomplish these additional feats because they fail to consider locational *and* attribute data concurrently. Only spatial statistics can provide this type of insight.

6. Discussion

In the course of this short report, two local spatial autocorrelation statistics have been introduced and applied to distributional archaeological data. At this point two questions should be raised: what does this analysis contribute to an understanding of the Classic Maya, and in what other archaeological contexts might local spatial statistics prove useful? These queries will be addressed in turn.

Whitley and Clark's [19] and Neiman's [12] analyses of trend surface residuals *assess the dissimilarity between individual terminal dates and interpolated expectations* as modeled by global and local polynomials, respectively. In contrast, the combined local spatial autocorrelation approach *assesses the similarity between each terminal date and those that fall within its local neighborhood and compares the sums of each neighborhood's values*. Thus, while trend surface residuals can be used to identify terminal dates that deviate from an interpolated global

expectation, I_i and G_i^* provide direct measures of how terminal dates deviate from those within a user-defined distance and how spatially defined neighborhoods of terminal dates compare to each other. Unlike those based on global analyses, locally based interpretations take multi-scale patterns of the global trend into consideration. In doing so, they add fine-grained details to a rather coarse-grained understanding of the behavioral processes responsible for patterns of spatial dependence in any archaeological assemblage of interest.

Local spatial autocorrelation results identify Classic Maya sites with terminal dates that are either much later than (e.g., Seibal) or much earlier than (e.g., Yaxha) terminal dates found at sites within spatially defined neighborhoods. Note that the prior statement contains information about how each terminal date fits into *local socio-political spheres* and *immediate biophysical surroundings*, while those afforded by global analyses state only whether each terminal date is later than or earlier than an interpolated expectation. Second, the discovery that the activity of monument building was largely coterminous among sites within two central neighborhoods illustrates the capability that local spatial autocorrelation statistics have to recognize spatial signatures left by human behaviors that operated at a scale larger than an individual site but smaller than the entire study area. This particular finding opens interpretation to numerous possibilities: that sites contained within some neighborhoods were each directly and detrimentally affected by a large-scale environmental or cultural stress due to their co-residence in a particular subregion of the southern Lowlands; that proximate sites were socially and economically interconnected to the extent that a small-scale stress experienced by one site indirectly affected many of its neighbors; or that a neighborhood's collective action of relinquishing monument building duties at roughly the same time was regulated by an institution that existed above the level of any individual site. Simply put, aspatial statistics are not qualified to justify such fine-grained hypotheses concerning spatial data. Furthermore, by uncovering possible avenues of research at the local level—where both aspatial and global spatial statistical techniques could not—it is apparent that local spatial statistics can help archaeologists tailor field projects to scales that are suitable for addressing primary research questions.

Local Moran's I_i and G_i^* have the ability to elucidate multi-scale landscape signatures in innumerable spatial data sets. It is beyond the scope of this paper to describe each and every archaeological context in which local spatial statistics might prove useful. At this time, archaeologists interested in using local methods to explore their own spatial data stand to gain more from a general discussion of relevant applications than from a laundry list of feasible projects. To achieve this type of generality, it is necessary to take a step back from the specifics

of the Maya example and discuss issues concerning *spatial scale*.

Spatial scale refers to the extent of a spatial phenomenon [18]. Any quantifiable attribute of an archaeological distribution can be referred to as a spatial phenomenon. Examples include quantity of lithic flakes, weight of ceramic sherds, quantity of Acheulian bifaces, and, as we saw above, terminal long-count dates of carved stone monuments. As a general rule, local Moran's I_i and G_i^* should prove useful in any context where assessments of spatial scale can be used to infer details of the processes responsible for an archaeological phenomenon's deposition. As was demonstrated in the case study, using local spatial statistics to quantify patterns that exist at a (theoretically infinite) number of scales between that of the artifact and that of the geographic region is as simple as varying the user-defined spatial lag distance, or "focusing" the lens through which spatial dependence is measured. Characterizing spatial autocorrelation throughout the entire range of possible lag distances provides a unique multi-scale perspective of the spatial dependence displayed by a single archaeological phenomenon which cannot be duplicated by other quantitative methods or by human perception.

The Maya case study explored one archaeological phenomenon for local spatial autocorrelation at numerous scales, but local spatial results also can be used to compare the degrees to which multiple archaeological phenomena display spatial dependence when analyzed at the same scale. For example, consider a hypothetical survey area in which each stone artifact is fashioned from one of only two raw material types, *A* or *B*. To infer something of the processes responsible for each raw material type's distinctive distribution, one could compare the degrees to which the quantities of *A* and *B* display patterns of spatial dependence at various scales. *Ceteris paribus*, archaeological phenomena that exhibit high levels of spatial dependence at considerably disparate scales are probably the results of either categorically different processes or similar processes which operated at quantitatively different scales, while comparable levels of spatial dependence displayed at comparable scales suggest that analogous processes were responsible for each assemblage. In the context of our hypothetical application, this multivariate local spatial analysis might provide additional clues as to how widely material types *A* and *B* were traded throughout the study area or which raw material type was used more expediently. Regardless of whether they are used to explore a single archaeological phenomenon for patterns via a multi-scale perspective or to compare the degrees of spatial dependence exhibited by multiple archaeological phenomena at the same scale, local spatial statistics offer intuitive quantitative methods for deciphering the spatial signatures of processes responsible for the formation of archaeological landscapes.

7. Conclusion

Despite the fact that many archaeological research questions involve significant spatial components, relatively few of the discipline's practitioners have employed spatial statistics in attempts to quantify landscape signatures in regional or intrasite material culture distributions. To be sure, notable exceptions exist, and the pioneering spatial autocorrelation studies reviewed above are among the best examples of those few archaeological applications. Yet, as a direct response to Kvamme's [8] now decade-old call to incorporate spatial statistics into the standard archaeological toolkit of quantitative methods, this paper finds little company in the recent literature. The computational potential of Geographic Information Systems (GIS), now literally at the fingertips of a growing number of archaeologists, provides the perfect opportunity for us to apply many of the techniques developed by our social science colleagues in quantitative geography to distributional archaeological data. For those who prefer not to work in a GIS, user-friendly statistical add-ins, like Rookcase, provide alternative means to sophisticated spatial analysis.

This report introduces archaeologists to quantitative methods that are more commonly employed by location-based investigations in related disciplines, such as geography and ecology. The analysis of an established archaeological data set from the southern Maya Lowlands demonstrates that local spatial statistics can inform refined interpretations of spatial data. A general discussion proposes that local spatial autocorrelation methods are capable of aiding archaeologists in many contexts, especially those in which a quantitative assessment of the scale at which an archaeological phenomenon displays spatial dependence can be used to infer details of the process(es) responsible for its formation. I encourage archaeologists to think about ways in which these methods could be applied to other distributional data sets in pursuit of answers to their own research questions. As demonstrated above, local spatial statistics show great promise, but, like many quantitative methods, their true utility to the discipline can only be measured by the quantity and diversity of the interpretations they benefit. It seems germane in closing to reiterate a portion of Williams' [20] optimistic prediction quoted at the onset, this time with an important modification: local spatial autocorrelation statistics should find many relevant archaeological applications.

Acknowledgements

I thank the Janet Upjohn Stearns Foundation for funding the majority of this research through an Independent Research Grant. What remained of the work

was supported by an Emil W. Haury Fellowship. Both sources of funding were awarded by the Department of Anthropology at the University of Arizona. I thank Brigitte Waldorf for introducing me to local spatial autocorrelation statistics and Gary Christopherson for encouraging me to apply them to archaeological research. This paper benefited from insightful comments by George Cowgill, Steve Kuhn, Mike Sawada, Jonathan Scholnick, Scott Van Keuren, Brigitte Waldorf, and two anonymous reviewers. While each of these individuals should be commended for improving the quality of this paper, I, alone, retain responsibility for deficiencies in presentation and/or logic.

References

- [1] L. Anselin, Local indicators of spatial autocorrelation—LISA, *Geographical Analysis* 27 (1995) 93–115.
- [2] F.J. Bove, Trend surface analysis and the Lowland Classic Maya collapse, *American Antiquity* 46 (1981) 93–112.
- [3] A.D. Cliff, J.K. Ord, *Spatial Autocorrelation*, Pion, London, 1973.
- [4] A. Getis, J.K. Ord, The analysis of spatial association by use of distance statistics, *Geographical Analysis* 24 (1992) 189–206.
- [5] P. Haggett, A.D. Cliff, A. Frey, *Locational Analysis in Human Geography 2: Locational Methods*, John Wiley, New York, 1977.
- [6] S.D. Houston, *Hieroglyphs and History at Dos Pilas: Dynastic Politics of the Classic Maya*, University of Texas Press, Austin, 1993.
- [7] K.L. Kvamme, Spatial autocorrelation and the Classic Maya collapse revisited, *Journal of Archaeological Science* 17 (1990) 197–207.
- [8] K.L. Kvamme, Spatial statistics and GIS: an integrated approach, in: J. Andresen, T. Madsen, I. Scollar (Eds.), *Computer Applications and Quantitative Methods in Archaeology*, Alden Press, Oxford, 1993, pp. 91–103.
- [9] J. Marcus, *Emblem and State and Classic Maya Lowlands: An Epigraphic Approach to Territorial Organization*, Dumbarton Oaks Research Library and Collection, Washington, 1976.
- [10] P. Moran, Notes on continuous stochastic phenomena, *Biometrika* 37 (1950) 17–23.
- [11] S.G. Morley, *The Inscriptions of Copan*, Carnegie Institute Publication, 219, Washington, 1920.
- [12] F.D. Neiman, Conspicuous consumption as wasteful advertising: a Darwinian perspective on spatial patterns in Classic Maya terminal monument dates, in: C. Barton, G. Clark (Eds.), *Rediscovering Darwin: Evolutionary Theory and Archaeological Explanation*, *Archaeological Papers of the American Anthropological Association*, 7, American Anthropological Association, Arlington, 1997, pp. 267–290.
- [13] J.K. Ord, A. Getis, Local spatial autocorrelation statistics: distributional issues and applications, *Geographical Analysis* 27 (1995) 286–306.
- [14] D.S. Rice, P.M. Rice, Physical geography, environment, and natural resources, in: J. Sabloff, J. Henderson (Eds.), *Late Lowland Maya Civilization in the Eighth Century A.D.*, Dumbarton Oaks Research Library and Collection, Washington, 1993, pp. 11–63.
- [15] M. Sawada, Rookcase: an Excel 97/ Visual Basic (VB) add-in for exploring global and local spatial autocorrelation, *Bulletin of the Ecological Society of America* 80 (1999) (2000) 231–234.

- [16] R.R. Sokal, N.L. Oden, B.A. Thomson, Local spatial autocorrelation in a biological model, *Geographical Analysis* 30 (1998) 331–354.
- [17] W.R. Tobler, A computer movie simulating urban growth in the Detroit region, *Economic Geography* 46 (1970) 234–240.
- [18] L. Wandsnider, Regional scale processes and archaeological landscape units, in: A.F. Ramenofsky, A. Steffen (Eds.), *Unit Issues in Archaeology*, University of Utah Press, Salt Lake City, 1998, pp. 87–102.
- [19] D.S. Whitley, W.A.V. Clark, Spatial autocorrelation tests and the Classic Maya collapse: methods and inferences, *Journal of Archaeological Science* 12 (1985) 377–395.
- [20] J.T. Williams, Spatial autocorrelation and the Classic Maya collapse: one technique, one conclusion, *Journal of Archaeological Science* 20 (1993) 705–709.